Parameter limits for neutrino oscillation with decoherence in KamLAND

G. Balieiro Gomes,[1,*] M. M. Guzzo,[1,†] P. C. de Holanda,[1,‡] and R. L. N. Oliveira[1,2,§]

[1]*Instituto de Física Gleb Wataghin, Universidade Estadual de Campinas—UNICAMP, Rua Sérgio Buarque de Holanda 777, 13083-970 Campinas, São Paulo, Brazil*

[2]*Universidade Federal do ABC - UFABC, Santo André, São Paulo, Brazil*

(Received 12 June 2014; revised manuscript received 13 April 2017; published 22 June 2017)

In the framework of open quantum systems, we analyze data from KamLAND by using a model that considers neutrino oscillation in a three-family approximation with the inclusion of the decoherence effect. Using a χ^2 test, we find new limits for the decoherence parameter, which we call γ, considering the most recent data by KamLAND. Assuming an energy dependence of the type $\gamma = \gamma_0(E/E_0)^n$, at a 95% C.L., the limits found are 3.7×10^{-24} GeV for $n = -1$, 6.8×10^{-22} GeV for $n = 0$, and 1.5×10^{-19} GeV for $n = 1$ on the energy dependence.

DOI: 10.1103/PhysRevD.95.113005

I. INTRODUCTION

In general, the study of vacuum neutrino oscillations is made in the framework of usual quantum mechanics, which considers the neutrino system to be isolated. In this work, we will do a different kind of analysis, in the framework of open quantum systems, considering the neutrinos, which will be our subsystem of interest, to have a coupling with the environment.

The theory of open quantum systems was created to deal with the case in which the system of interest is not considered isolated [1–3]. Instead, it has a coupling with the environment, and such coupling has important consequences for its evolution.

As we will see, the coupling with the environment will act to change the superposition of states, eliminating the coherence, similarly to what we have when a measurement is made in a quantum system, and generating a decoherence effect. We can find in the literature studies of the decoherence effect applied to neutrino oscillations [4–7].

Using this different approach to study neutrino oscillations, we see that different forms of the survival probability are obtained [4]. The goal of this work is to test one of these forms using data from the KamLAND experiment.

KamLAND [8–12] is a long baseline experiment, located at the Kamioka mine in Gifu, Japan, and it detects electron antineutrinos which come from nuclear reactors at an average distance of ∼180 km from the detector. It was constructed to test the so-called large mixing angle (LMA) solution to the solar neutrino problem, and its results were found to have a striking agreement with solar neutrino results [12].

The goal of this work is to obtain new limits for the parameter γ which describes decoherence, considering the most recent KamLAND data. We will also stress its relevance and the difference between the results found in this work and others, such as those from Ref. [7]. In Sec. II, we review the theory of open quantum systems, and we show how it can be used to study neutrino oscillations. We present how the decoherence effect arises, generating a different form of the survival probability, which is tested using a χ^2 test. The simulation results and the limits of the parameters are presented in Sec. III. We present our conclusions in Sec. IV.

II. FORMALISM

In this section, we will introduce the formalism used to obtain probabilities with dissipation effects from the Lindblad master equation. In this formalism, the neutrinos are treated as an open quantum system, and it interacts with the quantum environment. We assume that the quantum environment works as a reservoir. These two quantum states compose the global system, and from the interaction between neutrinos and environment arise the dissipation effects [1,2]. In open quantum system theory, it is possible to show that if the interaction between the subsystem of interest—which are the neutrinos in this case—and the reservoir is weak, the dynamic can be obtained by the Lindblad master equation [1,2]. A review of the fundamentals of quantum open system theory can be found in Refs. [1,2].

The Lindblad master equation can be written as [13,14]

$$\frac{d}{dt}\rho(t) = -i[H, \rho(t)] + D[\rho(t)], \tag{1}$$

with

$$D[\rho(t)] = \frac{1}{2}\sum_{k=1}^{N^2-1}([V_k, \rho(t)V_k^\dagger] + [V_k\rho(t), V_k^\dagger]), \tag{2}$$

where N is the dimension of the Hilbert space of the subsystem of interest and V_k describes the interaction between the subsystem of interest and the environment. In this equation, we see a term which is equal to the one we

*balieiro@ifi.unicamp.br
†guzzo@ifi.unicamp.br
‡holanda@ifi.unicamp.br
§robertol@ifi.unicamp.br

have in the Liouville equation, but we also have the term $D[\rho(t)]$, which appears because we are dealing with an open system, different from what we have in usual quantum mechanics, where the system is considered isolated. $D[\rho(t)]$ must satisfy some mathematical constraint, and then it can be phenomenologically parametrized.

We will impose on this equation the requirement that the entropy increase with time, so that $D[\rho(t)]$ evolves from a pure state asymptotically to a state of maximal mixing. Using the Von Neumann entropy, it is possible to show that this condition leads to restrictions on the operator V_k—in particular, we see that it must be Hermitian [15].

The Lindblad equation in (1) can be expanded in the basis of $SU(3)$ matrices, since the three neutrino families are considered in this work. In this form, each operator in Eq. (1) can be expanded as $O = a_\mu \lambda_\mu$, where λ are the Gell-Mann matrices. Then, the evolution equation in Eq. (1) can be written as

$$\frac{d}{dx}\rho_k(x) = 2\epsilon_{ijk}H_i\rho_j(x) + D_{kl}\rho_l(x), \tag{3}$$

and the probability conservation leads to $D_{\mu 0} = D_{0\nu} = 0$.

It is important to note that $\dot{\rho}_0(t) = 0$, and its solution is given by $\rho_0(t) = 1/N$, where N is the number of families. For simplicity, we do not include this component in the equation above.

There are many parameters in the dissipator matrix D_{kl}. However, it is possible to reduce the number of these parameters considerably if we impose some physical and mathematical constraints.

In order to obtain a dissipator matrix D_{kl} with parameters that describe well-known effects, we can impose first that $[H, V_k] = 0$. From the physical point of view, this commutation relation implies energy conservation in the neutrino subsystem, and this constraint also includes the decoherence effect in the evolution. This effect eliminates the quantum coherence, and the oscillation probability is changed by damping terms that are multiplied by oscillation terms. In this condition, the D_{kl} assumes the following form:

$$D_{kl} = -\text{diag}\{\gamma_{21}, \gamma_{21}, 0, \gamma_{31}, \gamma_{31}, \gamma_{32}, \gamma_{32}, 0\}, \tag{4}$$

where each γ_{ij} can describe the decoherence effect between the families i and j [5].

Once the neutrinos are free to interact with the reservoir, the energy in the neutrino sector can fluctuate, and hence the energy conservation constraint may not be satisfied. We can relax this constraint, adding two other new parameters in D, D_{33}, and D_{88}, such that the dissipator in Eq. (4) becomes

$$D_{kl} = -\text{diag}\{\gamma_{21}, \gamma_{21}, \gamma_{33}, \gamma_{31}, \gamma_{31}, \gamma_{32}, \gamma_{32}, \gamma_{88}\}, \tag{5}$$

where again γ_{ij} can describe the decoherence effect between the families i and j, while γ_{33} and γ_{88} describe the so-called relaxation effect.

The relaxation effect is a phenomenon that dynamically leads the states to their maximal mixing state. This phenomenon appears in the oscillation probabilities through the damping term multiplied by terms that depend only on mixing parameters. Then, when the relaxation effect is taken into account, the probabilities tend asymptotically to $1/N$, where N is the number of families initially considered.

In general, if a particular density matrix represents an initial physical state, the density matrix evolved by Eq. (1) may not be a well-defined quantum state. Complete positivity is a constraint on D_{kl} which always keeps the evolution made by Eq. (1) physical [2,16]. From complete positivity, the D_{kl} needs to be a positive matrix, and this is satisfied if the diagonal elements of D_{kl} are larger than the off-diagonal elements. So, we are going to consider the dissipator matrix obtained in Eq. (5) to evolve the neutrinos according to complete positivity, which corresponds to the most effective dissipator that we can obtain. Any other off-diagonal element can be represented in function of the main diagonal elements, since the γ_{33} and γ_{88} parameters are non-null.

The Hamiltonian in the effective mass basis can be written as

$$\tilde{H} = \frac{1}{2E}\begin{pmatrix} \tilde{m}_1^2 & 0 & 0 \\ 0 & \tilde{m}_2^2 & 0 \\ 0 & 0 & \tilde{m}_3^2 \end{pmatrix}, \tag{6}$$

with

$$\begin{aligned} \tilde{m}_1 &= -\frac{1}{2}((\delta\cos 2\theta_{12} - A\cos^2\theta_{13})^2 + \delta^2\sin^2 2\theta_{12})^{\frac{1}{2}}, \\ \tilde{m}_2 &= \frac{1}{2}((\delta\cos 2\theta_{12} - A\cos^2\theta_{13})^2 + \delta^2\sin^2 2\theta_{12})^{\frac{1}{2}}, \end{aligned} \tag{7}$$

where $\delta = m_2^2 - m_1^2$, $A = 2\sqrt{2}n_e E\cos^2\theta_{13}$, and

$$\tilde{m}_3 = \frac{1}{2}(2m_3^2 - m_2^2 - m_1^2 + A\sin^2\theta_{13}). \tag{8}$$

The relation between the flavor state and the effective mass basis is given by the following transformation:

$$\rho_\alpha = U\rho_{\tilde{m}}U^\dagger = U_{13}\tilde{U}_{12}\rho_{\tilde{m}}\tilde{U}_{12}^\dagger U_{13}^\dagger, \tag{9}$$

where the ρ_α is the flavor state and $\rho_{\tilde{m}}$ is the effective mass state. The mixing matrix U is explicitly defined as

$$U = \begin{pmatrix} \cos\theta_{13} & 0 & \sin\theta_{13} \\ 0 & 0 & 0 \\ -\sin\theta_{13} & 0 & \cos\theta_{13} \end{pmatrix}\begin{pmatrix} \cos\tilde{\theta}_{12} & \sin\tilde{\theta}_{12} & 0 \\ -\sin\tilde{\theta}_{12} & \cos\tilde{\theta}_{12} & 0 \\ 0 & 0 & 1 \end{pmatrix}, \tag{10}$$

and the effective mixing angle has the usual form

$$\sin^2 2\tilde{\theta}_{12} = \frac{\delta^2 \sin^2 2\theta}{(\delta \cos 2\theta_{12} - A\cos^2\theta_{13})^2 + \delta^2 \sin^2 2\theta_{12}}. \quad (11)$$

We have defined a diagonal form to the Hamiltonian in Eq. (6). Hence, the dissipators in Eqs. (4) and (5) remain diagonal as well.

The evolved density matrix in the effective mass basis is given by

$$\rho_{\tilde{m}}(x) = \begin{pmatrix} \rho_{11}(x) & \rho_{12}(0)e^{-\tilde{\Delta}^*_{12}x} & \rho_{13}(0)e^{-\tilde{\Delta}^*_{13}x} \\ \rho_{21}(0)e^{-\tilde{\Delta}_{12}x} & \rho_{22}(x) & \rho_{23}(0)e^{-\tilde{\Delta}_{23}x} \\ \rho_{31}(0)e^{-\tilde{\Delta}_{13}x} & \rho_{32}(0)e^{-\tilde{\Delta}^*_{23}x} & \rho_{33}(x) \end{pmatrix}, \quad (12)$$

where $\rho_{ij}(0)$ are elements of the initial state obtained from Eq. (10) and $\tilde{\Delta}_{ij} = \gamma_{ij} + i(\tilde{m}_i^2 - \tilde{m}_j^2)/2E$. While the ρ_{ii} elements are given by

$$\begin{aligned} \rho_{11}(x) &= \frac{1}{3} + \frac{1}{2}e^{-\gamma_{33}x}\cos 2\tilde{\theta}_{12}\cos^2\theta_{13} \\ &\quad - \frac{1}{12}e^{-\gamma_{88}x}(1 - 3\cos 2\theta_{13}), \\ \rho_{22}(x) &= \frac{1}{3} - \frac{1}{2}e^{-\gamma_{33}x}\cos 2\tilde{\theta}_{12}\cos^2\theta_{13} \\ &\quad - \frac{1}{12}e^{-\gamma_{88}x}(1 - 3\cos 2\theta_{13}), \\ \rho_{33}(x) &= \frac{1}{3} + \frac{1}{6}e^{-\gamma_{88}x}(1 - 3\cos 2\theta_{13}). \end{aligned} \quad (13)$$

These damping terms in the diagonal elements describe the relaxation effect through the parameters γ_{33} and γ_{88}. Besides that, they depend on the mixing parameters θ_{12} and θ_{13} and the distance between the source and the detection point. The main diagonal in state (12) can be interpreted as the probabilities to find $\tilde{m}_1$, $\tilde{m}_2$, or $\tilde{m}_3$ of the observable H in Eq. (6). In usual quantum mechanics, these elements do not change within an adiabatic propagation. So, by analyzing the state in (12), we can see how the relaxation effect acts on the probabilities.

The state in (12) shows how the relaxation effect depends on the propagation distance. Considering the Mikheyev-Smirnov-Wolfenstein (MSW) solution for solar neutrinos, which produces a specific relation between mass eigenstates in the final neutrino flux, we expect that the relaxation effects are strongly constrained. We will present this analysis somewhere else, but the Sun-Earth distance is of the order of 10^{17} eV^{-1}, and a rough limit for both relaxation parameters is 10^{-18} eV, in order to have $\exp[-\gamma_{ii}x] \sim 1$. Thus, the analysis of reactor neutrinos can disregard the relaxation effect because the larger baseline to this source is much smaller than the Sun-Earth distance.

The off-diagonal elements are known as coherence elements. In state (12), these elements tend to zero during the propagation due to the damping terms. This is the exact definition of the decoherence effect. But, in the solar neutrino context, these elements are averaged out, and any decoherence effect information is lost if we consider a model-independent approach [17]. Besides, since $|\Delta m^2_{13}| \sim |\Delta m^2_{23}| \gg |\Delta m^2_{12}|$, experiments such as KamLAND, that are tuned to test Δm^2_{12}, are not sensible to the coherence elements ρ_{i3}. These elements depend on $\tilde{\Delta}_{i3}x$ with $i \neq 3$, which oscillate very fast, and hence are averaged out.

So, disregarding the fast-oscillating terms and the relaxation effects, the state is given by

$$\rho_{\tilde{m}}(x) = \begin{pmatrix} \rho_{11}(0) & \rho_{12}(0)e^{-\tilde{\Delta}^*_{12}x} & 0 \\ \rho_{21}(0)e^{-\tilde{\Delta}_{12}x} & \rho_{22}(0) & 0 \\ 0 & 0 & \rho_{33}(0) \end{pmatrix}, \quad (14)$$

and using Eq. (10) to write the state above in the flavor basis, the survival probability can be obtained by taking

$$P_{\nu_\alpha \to \nu_\alpha} = \mathrm{Tr}[\rho_\alpha(0)\rho_\alpha(t)], \quad (15)$$

where the initial state for $\bar{\nu}_e$ is $\rho_\alpha(0) = \mathrm{diag}\{1, 0, 0\}$. So, the survival probability is given by [11]

$$P^{3\nu}_{\nu_\alpha \to \nu_\alpha} = \cos^4(\theta_{13})\tilde{P}^{2\nu}_{\nu_\alpha \to \nu_\alpha} + \sin^4(\theta_{13}), \quad (16)$$

where $\tilde{P}^{2\nu}_{\nu_\alpha \to \nu_\alpha}$ is written

$$\tilde{P}^{2\nu}_{\nu_\alpha \to \nu_\alpha} = 1 - \frac{1}{2}\sin^2(2\tilde{\theta}_{12})\left[1 - e^{-\gamma x}\cos\frac{(\tilde{m}_1^2 - \tilde{m}_2^2)}{2E}x\right], \quad (17)$$

which is the same probability obtained in a two-neutrino approximation when the decoherence effect is taken into account [17].

It is important to explain the difference between the analysis made in this work and the one made in Ref. [7], where they use a different set of data from KamLAND (older than the one considered here), but also consider data from solar neutrinos.

The first difference is that we are dealing with three neutrino families. Moreover, as shown in Ref. [4] and mentioned before, there are cases in which, besides the decoherence effect, other effects arise from the coupling with the environment, such as the so-called relaxation effect [4]. Since in our case, as previously shown, decoherence is the only relevant effect in the interaction with the environment, including solar neutrinos in the analysis would not bring any new information regarding the decoherence parameter. Solar neutrinos cannot be used to bound decoherence, because the fast-oscillating terms in $\tilde{\Delta}_{ij}x$ average out all the coherence terms [17,18]. Therefore, the effect studied here is different from the one studied in Ref. [7]. According to Ref. [17], the limits found in Ref. [7] are combined limits on relaxation and decoherence effects in a model-dependent approach. We use a model-independent approach in this paper to analyze the KamLAND data.

TABLE I. Best-fit results For three free parameters.

	$n=0$	$n=1$	$n=-1$
χ^2_{min}	21.44	21.92	21.03
Δm^2	$8.05\times10^{-5}\,\text{eV}^2$	$8.05\times10^{-5}\,\text{eV}^2$	$8.05\times10^{-5}\,\text{eV}^2$
$\tan^2(\theta)$	0.44	0.42	0.47
γ_0	$2.37\times10^{-22}\,\text{GeV}$	$4.14\times10^{-20}\,\text{GeV}$	$1.17\times10^{-24}\,\text{GeV}$

III. RESULTS

We used the set of data presented in Ref. [11], where the data is presented in 20 energy bins. For this set of data, we tested the usual oscillation scenario, and found for the best-fit point $\chi^2_{\text{min}}=22.96$, $\Delta m^2_{12}=8.05\times10^{-5}\,\text{eV}^2$, $\tan^2(\theta_{12})=0.40$. We can see that χ^2_{min} is close to the number of degrees of freedom, indicating a good agreement with the experimental data.

We consider now the oscillation probability in Eq. (17) with the three-family approximation [Eq. (21)] and the three free parameters Δm^2_{12}, $\tan^2(\theta_{12})$, and γ, also considering a possible energetic dependence on γ:

$$\gamma=\gamma_0\left(\frac{E}{E_0}\right)^n, \tag{18}$$

with $E_0=1$ GeV, such as the one done by Ref. [7]. We did this test for $n=0$, $n=1$, and $n=-1$. We also considered the best-fit value for θ_{13} given by Ref. [19], $\sin^2(2\theta_{13})=9.3\times10^{-2}$.

The best-fit results for these scenarios can be seen in Table I for the three values of n, where again we see that the value of χ^2_{min} is close to the number of degrees of freedom.

We can also see that including the third parameter γ slightly improves the fit in comparison with the scenario where $\gamma=0$, with a decrease in the value of χ^2_{min}.

We present confidence level curves for $n=0$ in the energy dependence, which can be seen in Figs. 1, 2 and 3, and in accordance with Ref. [19] we chose the values of $\Delta\chi^2$ to get confidence levels of 68.27%, 90%, 95%, 99%, and 99.73%.

For $n=1$ in the energy dependence, the confidence level curves obtained are given in Figs. 4, 5, and 6, and for

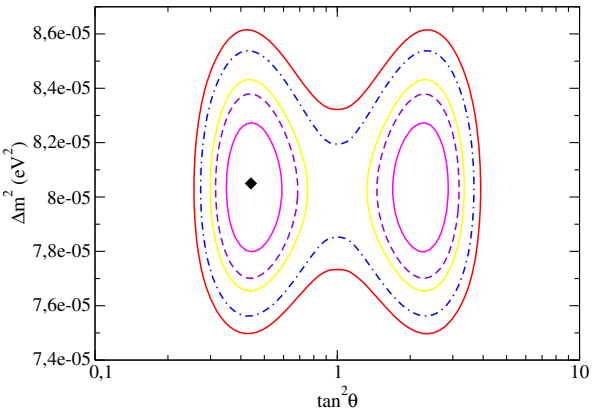

FIG. 1. Confidence level curves for $n=0$. The curves correspond to 68.27%, 90%, 95%, 99%, and 99.73% C.L.

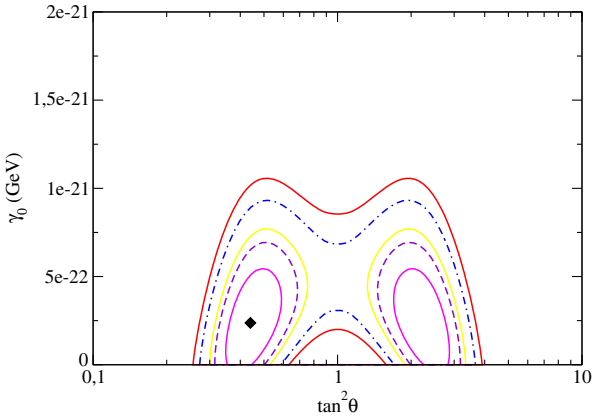

FIG. 2. Confidence level curves for $n=0$. The curves correspond to 68.27%, 90%, 95%, 99%, and 99.73% C.L.

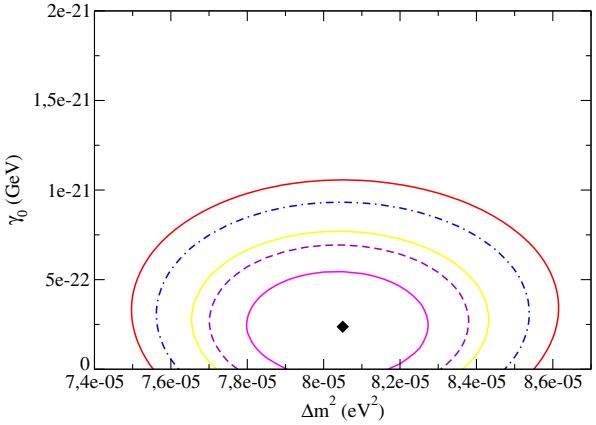

FIG. 3. Confidence level curves for $n=0$. The curves correspond to 68.27%, 90%, 95%, 99%, and 99.73% C.L.

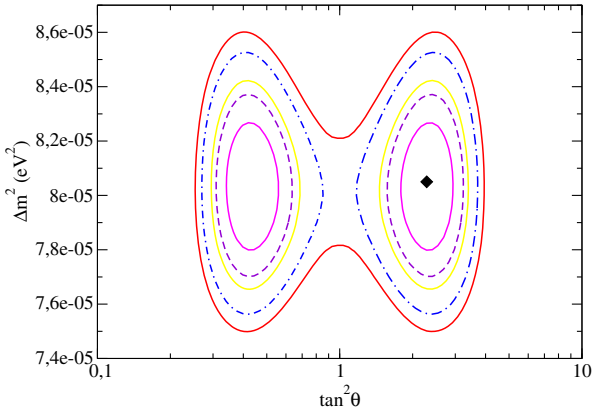

FIG. 4. Confidence level curves for $n=1$. The curves correspond to 68.27%, 90%, 95%, 99%, and 99.73% C.L.

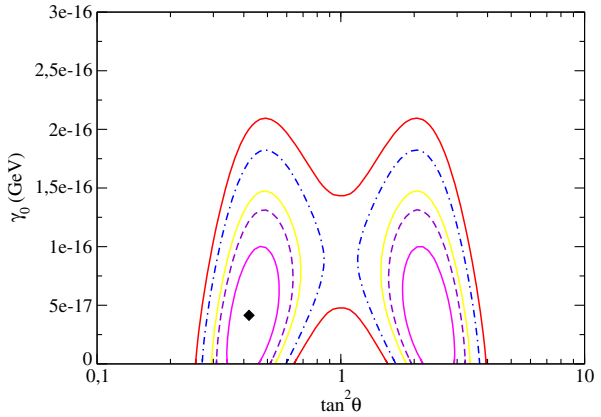

FIG. 5. Confidence level curves for $n = 1$. The curves correspond to 68.27%, 90%, 95%, 99%, and 99.73% C.L.

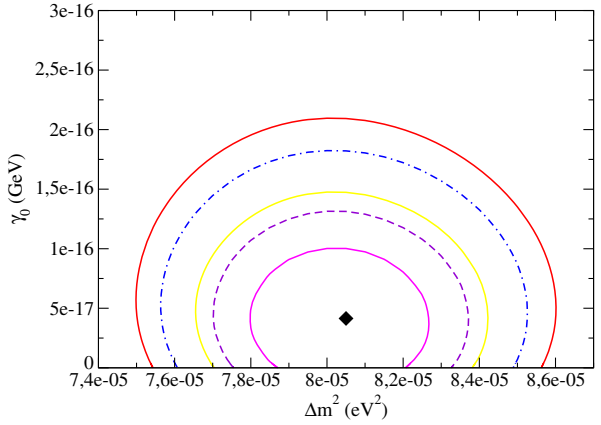

FIG. 6. Confidence level curves for $n = 1$. The curves correspond to 68.27%, 90%, 95%, 99%, and 99.73% C.L.

$n = -1$ in the energy dependence, the confidence level curves obtained are given in Figs. 7, 8, and 9.

We can see from Figs. 1–9 that the decoherence effect does not alter the value of the best-fit point for Δm^2, which

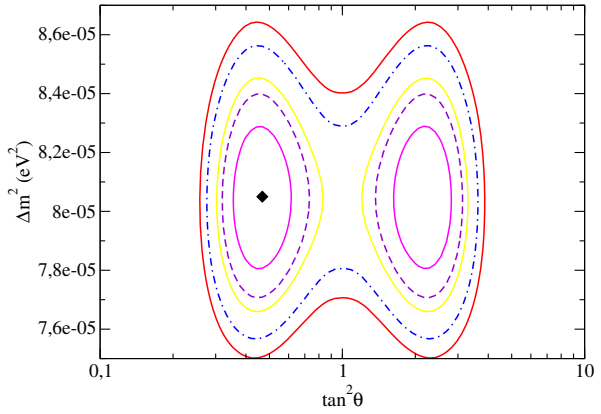

FIG. 7. Confidence level curves for $n = -1$. The curves correspond to 68.27%, 90%, 95%, 99%, and 99.73% C.L.

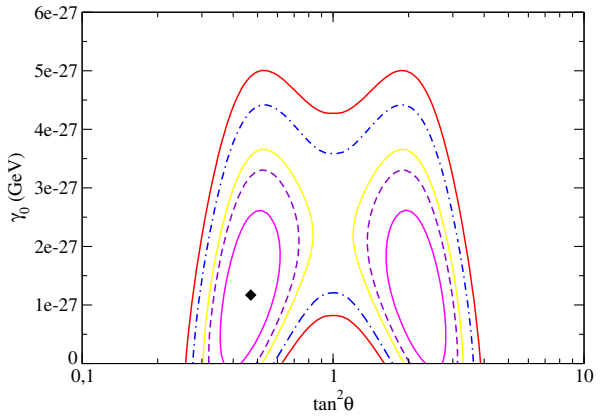

FIG. 8. Confidence level curves for $n = -1$. The curves correspond to 68.27%, 90%, 95%, 99%, and 99.73% C.L.

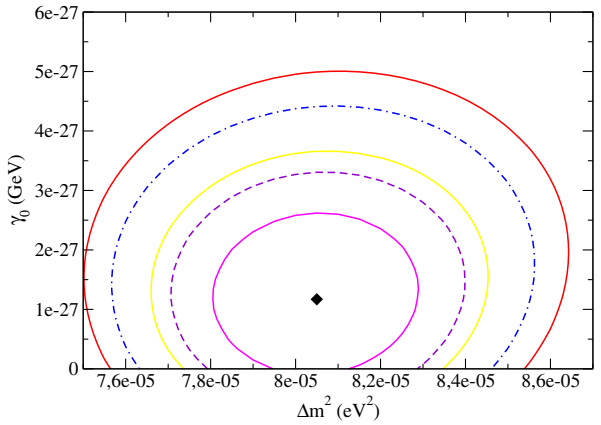

FIG. 9. Confidence level curves for $n = -1$. The curves correspond to 68.27%, 90%, 95%, 99%, and 99.73% C.L.

is consistent with our previous analysis, since the damping term depending on γ acts only on the amplitude of the survival probability.

From the confidence level curves of Figs. 1–9, we can obtain limits for the oscillation parameters and for γ_0, the decoherence parameter. For 95% C.L., the upper limits on γ_0 are given in Table II.

In order to visualize the effect of the inclusion of decoherence in our study of neutrino oscillations, we can reproduce an important graph originally presented by the KamLAND Collaboration.

Following the same procedure used by KamLAND, we used our results to make Fig. 10, which is the result of merging the original graph [11] and the graph we made for oscillation with decoherence.

TABLE II. Upper limits for γ_0 at a 95% C.L. with $n = 0, 1, -1$.

$n = -1$	3.7×10^{-24} GeV
$n = 0$	6.8×10^{-22} GeV
$n = 1$	1.5×10^{-19} GeV

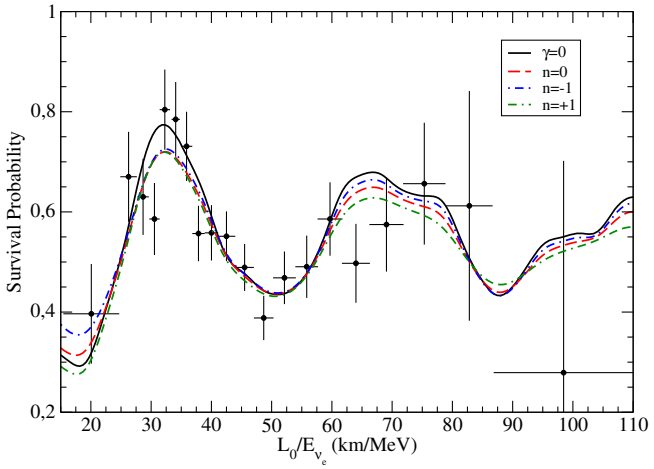

FIG. 10. Graph made with data from the simulation of our model for oscillation with decoherence considering best-fit values of the three parameters and the three different values for n in the energy dependence. We also include the KamLAND data [11].

In Fig. 10, we can see that the fit of the data made from our model of oscillation with decoherence is a good fit of the data, showing a visual confirmation of the analysis provided by the χ^2 test.

We see that the inclusion of decoherence causes a damping on the oscillation pattern, as we already expected from our theoretical predictions. We can also see that this damping is not too strong for the values of the decoherence parameter best-fit points.

IV. CONCLUSION

In this work, we treated the appearance of the decoherence effect on neutrino oscillations in a phenomenological approach, studying first open quantum systems in general, and then applying the results to the case of neutrino oscillation in three families. We analyzed the constraints in the model parameters coming from a fit to KamLAND data.

The results were obtained when we considered the most recent set of KamLAND data, provided by Ref. [11], where the number of events were presented in 20 bins. Comparing the value of χ^2_{min} with the number of degrees of freedom, we saw that including the third parameter, γ, improves the fit of the data. With $\gamma = 0$, we obtained $\chi^2_{\text{min}} = 22.96$, and for γ as a free parameter (hence 20 experimental points and 3 parameters), we obtained a decrease for χ^2_{min} of order $\Delta\chi^2 \sim 1$. These results are summarized in Table I. We also found a best-fit value with $\gamma \neq 0$.

To support the results of our analysis, giving a more visual way of evaluating the results, we reproduced a graph originally presented by the KamLAND Collaboration, which showed the survival probability versus L_0/E, which shows clearly the oscillation pattern for the neutrinos.

Comparing the original graph with our reproduction, which was made using the best-fit values obtained in our simulation, we saw that our model provided a fit of the data which was indeed in agreement with the experiment uncertainties, as can be seen in Fig. 10.

We also determined new limits for γ_0 at a 95% C.L. The limits are presented in Table II, and were determined based on the confidence level curves made from the most recent set of Kamland data [11].

ACKNOWLEDGMENTS

The authors would like to thank FAPESP, CAPES, and CNPq for their financial support.

[1] H. P. Breuer and F. Petruccione, *The Theory of Open Quantum Systems*, Lecture Notes in Physics (Oxford University Press, New York, 2002).
[2] R. Alicki and K. Lendi, *Quantum Dynamical Semigroups and Applications*, Lecture Notes in Physics (Springer-Verlag, Berlin, 1987).
[3] J. Ellis, J. S. Hagelin, D. V. Nanopoulos, and M. Srednicki, Nucl. Phys. **B241**, 381 (1984).
[4] R. L. N. Oliveira and M. M Guzzo, Eur. Phys. J. C **69**, 493 (2010).
[5] R. L. N. Oliveira and M. M. Guzzo, Eur. Phys. J. C **73**, 2434 (2013).
[6] R. L. N. Oliveira, M. M. Guzzo, and P. C. de Holanda, Phys. Rev. D **89**, 053002 (2014).
[7] G. L. Fogli, E. Lisi, A. Marrone, D. Montanino, and A. Palazzo, Phys. Rev. D **76**, 033006 (2007).
[8] K. Eguchi *et al.* (KamLAND Collaboration), Phys. Rev. Lett. **90**, 021802 (2003).
[9] S. Abe *et al.* (KamLAND Collaboration), Phys. Rev. C **81**, 025807 (2010).
[10] S. Abe *et al.* (KamLAND Collaboration), Phys. Rev. Lett. **100**, 221803 (2008).
[11] A. Gando *et al.* (KamLAND Collaboration), Phys. Rev. D **83**, 052002 (2011).
[12] K. Eguchi *et al.* (KamLAND Collaboration), Phys. Rev. Lett. **90**, 021802 (2003).
[13] V. Gorini and A. Kossakowski, J. Math. Phys. (N.Y.) **17**, 821 (1976).
[14] G. Lindblad, Communications in Physics **48**, 119 (1976).
[15] F. Benatti and H. Narnhofer, Lett. Math. Phys. **15**, 325 (1988).

[16] F. Benatti and R. Floreanini, J. High Energy Phys. 02 (2000) 32.
[17] M. M. Guzzo, P. C. de Holanda, and R. L. N. Oliveira, Nucl. Phys. **B908**, 408 (2016).
[18] P. Bakhti, Y. Farzan, and T. Schwetz, J. High Energy Phys. 05 (2015) 007.
[19] K. A. Olive *et al.* (Particle Data Group Collaboration), Chin. Phys. C **38**, 090001 (2014).